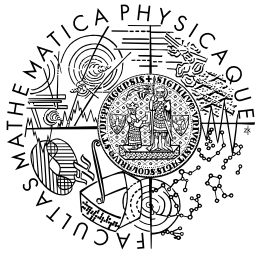

FACULTY
OF MATHEMATICS
AND PHYSICS
Charles University

BACHELOR THESIS

Oleksandr Kornijčuk

Computations of Laguerre tessellations with given cell volumes

Department of Probability and Mathematical Statistics

Supervisor of the bachelor thesis: prof. RNDr. Viktor Beneš, DrSc.
Study programme: Mathematics
Study branch: General Mathematics

Prague 2022

I declare that I carried out this bachelor thesis independently, and only with the cited sources, literature and other professional sources. It has not been used to obtain another or the same degree.

I understand that my work relates to the rights and obligations under the Act No. 121/2000 Sb., the Copyright Act, as amended, in particular the fact that the Charles University has the right to conclude a license agreement on the use of this work as a school work pursuant to Section 60 subsection 1 of the Copyright Act.

In ..... date ....

Author's signature

Above all, I want to express my gratitude to prof. RNDr. Beneš Viktor, DrSc. for his invaluable advice, guidance, and patience, which helped me complete this thesis. I would also like to thank Mgr. Seitl Filip for his consultations on the application and usage of the Voro++ library. Additionally, my gratitude extends to professor Chris H. Rycroft at the University of Wisconsin-Madison, who has created and maintained the Voro++ library.

Title: Computations of Laguerre tessellations with given cell volumes

Author: Oleksandr Kornijčuk

Department: Department of Probability and Mathematical Statistics

Supervisor: prof. RNDr. Viktor Beneš, DrSc., Department of Probability and Mathematical Statistics

Abstract: Given a finite set of pairs in $\mathbb{R}^d \times \mathbb{R}$, nuclei and weights, Laguerre tessellations allow us to subdivide Euclidean space $\mathbb{R}^d$ into finitely many polyhedral cells using the power distance. We are interested in the problem of finding weights so that the Laguerre cells have prescribed volumes and nuclei. Our primary aim is to present the theoretical background leading to the problem's solution. Here we complete some proofs that are shortened in the literature, while other theorems are cited. Then, we demonstrate two own computer programs and the corresponding numerical results. First, we compute the desired set of weights that generates the Laguerre tessellation with prescribed cell volumes and apply it to a unit cube in $\mathbb{R}^3$. The application of this method relies on the Barzilai-Borwein gradient descent and Voro++ library, which computes the volumes of cells in each iteration. Furthermore, an iterative approach approximates a centroidal Laguerre tessellation, where the nuclei coincide with the centroids of Laguerre cells.

Keywords: Laguerre tessellation, assignment, capacity, Barzilai-Borwein algorithm

Contents

Introduction

This thesis aims to provide an introduction to the problem of Laguerre tessellations and a structured approach to generating Laguerre tessellations with prescribed cell volumes. We follow Aurenhammer et al. [1998] while providing proof of some parts that the authors assumed to be trivial.

Next, to provide a practical example of our theoretical results, we implement an algorithm to compute Laguerre tessellations with given cell volumes using an iterative approach from Aurenhammer et al. [1998], step optimization from Kuhn et al. [2020], and a specialized library for three-dimensional computations of Laguerre tessellations Voro++, see Rycroft [2009].

There are different approaches to Laguerre tessellations; hence, our definitions and notation might not be general. Throughout the text, we work in the Euclidean space $\mathbb{R}^d$ with norm $\|\cdot\|$ and standard scalar product $\langle\cdot,\cdot\rangle$. First, we need to prove the existence of those tessellations. Hence, we must lay the theoretical groundwork to explore more complex ideas.

Definition 1. *Let $m \in \mathbb{N}$ and let us consider a set $N = \{n_1, \ldots, n_m\}$ of elements in $\mathbb{R}^d$, which we will call nuclei, and a set $W = \{w_1, \ldots, w_m\}$ of elements in $\mathbb{R}$, which we will call weights (associated with the nuclei).*

Remark. Later we will need an interpretation $w_i = r_i^2$, r_i being a radius of a sphere centered in n_i. Since w_i can be negative, the notion of an imaginary sphere can be considered. A sphere with an imaginary radius $r' = ir,\ r \geq 0$, where i is the imaginary unit, is called an imaginary sphere, see Aurenhammer [1987], p. 51. A sphere with either a real or imaginary radius is called a generalized sphere.

Definition 2. *Let us consider the sets N and W from Definition 1. We define a mapping $p_W \colon \mathbb{R}^d \times N \to \mathbb{R}$, which we shall call the power function, as*

$$p_W(x, n_i) = \|x - n_i\|^2 - w_i \text{ for all } x \in \mathbb{R}^d \text{ and } i = 1, \ldots, m. \tag{1}$$

Remark. Formula (1) is also called the power distance of x from (n_i, w_i), see Lautensack and Zuyev [2008], p. 631. The definition of power function requires the set of nuclei and the set of weights; however, we only use W to describe p_W. We do it because the set of nuclei N will be fixed, and only W will vary.

We selected a finite set of nuclei in $\mathbb{R}^d$, and we created a way to measure the relationship between points in $\mathbb{R}^d$ and nuclei in N other than $\|\cdot\|$. A particular subdivision of $\mathbb{R}^d$ arises.

Definition 3. *Let us consider the sets N and W from Definition 1. Let us also consider a subset of $\mathbb{R}^d$ that consists of all points in $\mathbb{R}^d$ closer to $n_i \in N$ (with respect to the power distance p_W) than any other nucleus in N and denote it by $reg_W(n_i)$. Those regions define an assignment $A_W \colon \mathbb{R}^d \to N$ given by*

$$A_W(x) = n_i \iff x \in reg_W(n_i),$$

i.e., $A_W^{-1}(n_i) = reg_W(n_i)$. The Laguerre tessellation of $\mathbb{R}^d$ with nuclei N and weights W is the collection of nonempty sets $reg_W(n_i)$ for $i = 1, \ldots, m$.

Remark. Laguerre tessellations are alternatively called power diagrams, see Aurenhammer [1987], p. 50. If we set all $w_i = 0$, the geometry of regions $\mathrm{reg}_W(n_i)$ depends solely on the position of nuclei, and we obtain the so-called Voronoi tessellation.

Remark. Definition 3 is ambiguous regarding the points at the same power distance from two different nuclei. Later we would like A_W to be Borel measurable. Hence, we select all points at the same power distance from two different nuclei and assign them to one fixed nucleus, say n_1.

Another (almost equivalent) definition of Laguerre tessellations exists that remedies this ambiguity. However, this definition does not induce the assignment A_W from Definition 3.

Definition 4. *Let us consider the sets N and W from Definition 1. For each nucleus $n_i \in N$ we define its cell as*

$$B_i = \{x \in \mathbb{R}^d : \ p_W(x, n_i) \leq p_W(x, n_j), \ j = 1, \ldots, m\}.$$

The collection of cells $B_1, \ldots, B_m$ is then called the Laguerre tessellation of $\mathbb{R}^d$ with nuclei N and weights W.

Remark. The cells from Definition 4 are convex closed sets with mutually disjoint interiors such that $\bigcup_{i=1}^m B_i = \mathbb{R}^d$; some cells might be empty, and a nucleus need not lie in its cell, see Lautensack and Zuyev [2008], p. 631–635.

Next, we focus on a d-dimensional unit hypercube in $\mathbb{R}^d$ and define a method of measuring the regions from Definition 3.

Definition 5. *Let $(\mathbb{R}^d, \mathcal{B}^d, \mu)$ be a probability space where μ is absolutely continuous with respect to the Lebesgue measure λ^d and its probability density function ρ is continuous and nonzero in $[0,1]^d$, and $\rho = 0$ outside $[0,1]^d$. Let us consider the assignment A_W from Definition 3. For each nucleus $n_i \in N$, we define the capacity of n_i resulting from A_W as $\mu(A_W^{-1}(n_i))$.*

Having formulated sufficient definitions, we can state the problem preoccupying us in the first chapter.

Claim 1. *Let us consider N from Definition 1 and μ satisfying Definition 5. For any set $C = \{C_1, \ldots, C_m\}$ of elements in $[0,1]$ such that $\sum_{i=1}^m C_i = 1$, there is a set of weights W for which we have*

$$\mu(reg_W(n_i)) = C_i, \ i = 1, \ldots, m,$$

i.e., there is a set W such that the Laguerre tessellation of $\mathbb{R}^d$ with nuclei N and weights W satisfies the prescribed capacity constraint C with respect to μ.

1. Theoretical Groundwork

In the following chapter, we provide a theoretical groundwork that enables us to justify our claim in the introduction and compute Laguerre tessellations with given cell volumes.

1.1 Existence

First, we prove that A_W from Definition 3 minimizes the mean squared Euclidean distance between points in $\mathbb{R}^d$ and nuclei in N over all Borel measurable assignments that satisfy a specific capacity constraint with respect to μ.

Lemma 2. *Let us consider the sets N and W from Definition 1 and μ from Definition 5. The assignment $A_W\colon \mathbb{R}^d \to N$ as defined in Definition 3 minimizes*

$$\int_{[0,1]^d} \rho(x)\ \|x - A(x)\|^2\ dx$$

over all Borel measurable $A\colon \mathbb{R}^d \to N$ with capacities $\mu(A_W^{-1}(n_i)),\ i = 1, \dots, m$.

Proof. For $i, j \in \{1, \dots, m\}$ such that $i \neq j$, we have

$$A_W^{-1}(n_i) \cap A_W^{-1}(n_j) = \emptyset,$$

and we see that

$$\bigcup_{i=1}^{m} A_W^{-1}(n_i) = \mathbb{R}^d.$$

By definition, A_W minimizes

$$\int_{\mathbb{R}^d} \rho(x)\ p_W(x, A(x))\ dx$$

over all Borel measurable $A\colon \mathbb{R}^d \to N$, since it chooses the closest points in $\mathbb{R}^d$ to a nucleus $n_i \in N$ with respect to the power distance p_W. Because $\rho = 0$ outside $[0,1]^d$, we see that

$$\int_{\mathbb{R}^d} \rho(x)\ p_W(x, A_W(x))\ dx = \int_{[0,1]^d} \rho(x)\ p_W(x, A_W(x))\ dx. \tag{1.1}$$

We know that

$$\int_{\mathbb{R}^d} \rho(x)\ p_W(x, A_W(x))\ dx = \int_{\mathbb{R}^d} \rho(x)\ \Big(\|x - A_W(x)\|^2 - \omega(A_W(x))\Big)\ dx,$$

where $\omega\colon N \to W$ assigns a nucleus its weight. By linearity of the Lebesgue integral, we see that

$$\int_{\mathbb{R}^d} \rho(x)\ \omega(A_W(x))\ dx = \sum_{i=1}^{m} \int_{A_W^{-1}(n_i)} \rho(x)\ \omega(A_W(x))\ dx. \tag{1.2}$$

For each $x \in A_W^{-1}(n_i)$, we have $A_W(x) = n_i$. Hence, (1.2) becomes

$$\sum_{i=1}^{m} w_i \int_{A_W^{-1}(n_i)} \rho(x)\ dx = \sum_{i=1}^{m} w_i\ \mu(A_W^{-1}(n_i)).$$

Since we only consider the assignments that satisfy the capacity constraint, the last expression is equal to some constant $K \in \mathbb{R}$. Therefore,

$$\int_{\mathbb{R}^d} \rho(x)\ p_W(x, A_W(x))\ dx = \int_{\mathbb{R}^d} \rho(x)\ \|x - A_W(x)\|^2\ dx - K.$$

From (1.1), it follows that

$$\int_{\mathbb{R}^d} \rho(x)\ p_W(x, A_W(x))\ dx + K = \int_{[0,1]^d} \rho(x)\ \|x - A_W(x))\|^2\ dx. \tag{1.3}$$

Thus, A_W also minimizes the right-hand side of (1.3), which yields the lemma. □

Without proof, the last lemma is stated as Lemma 2 in Aurenhammer et al. [1998], p. 65. It is helpful to define particular classes of assignments that simplify discussing Laguerre tessellations at this point.

Definition 6. *Let us consider N from Definition 1 and μ from Definition 5. We call a Borel measurable $A\colon \mathbb{R}^d \to N$ a least-square assignment if it minimizes*

$$\int_{\mathbb{R}^d} \rho(x)\ \|x - A(x)\|^2\ dx \tag{1.4}$$

over all Borel measurable assignments $\mathbb{R}^d \to N$.

Definition 7. *Let us consider N from Definition 1, μ satisfying Definition 5 and a set $C = \{C_1, \ldots, C_m\}$ of elements in $[0, 1]$ such that $\sum_{i=1}^{m} C_i = 1$. We call a Borel measurable $L\colon \mathbb{R}^d \to N$ a least-square assignment subject to the capacity constraint C, if it is a least-square assignment and*

$$C_i = \mu(L^{-1}(n_i)),\ i = 1, \ldots, m,$$

i.e., it minimizes (1.4) over all Borel measurable assignments $\mathbb{R}^d \to N$ that satisfy the capacity constraint C.

Remark. Assignments defined by Laguerre tessellations are least-square assignments subject to the capacity resulting from the assignment by Lemma 2.

Next, we show a specific geometric property of least-square assignments subject to some capacity constraint.

Lemma 3. *Let us consider N, μ and C from Definition 7. Let us assume that there exists a least-square assignment L subject to C. Then for all $n_i, n_j \in N$ such that $i \neq j$ there exists a hyperplane θ in $\mathbb{R}^d$ orthogonal to $(n_j - n_i)$ such that*

$$\mu(\theta_{ij} \cap L^{-1}(n_j)) = 0 \text{ and } \mu(\theta_{ji} \cap L^{-1}(n_i)) = 0,$$

where θ_{ij} is the closed halfspace bounded by θ and containing $\theta + (n_i - n_j)$, and θ_{ji} is the complementary halfspace.

Proof. In the following proof, the variable of integration in each integral is x. Since the range of L is finite, we see that (1.4) is equal to

$$L(x) = \sum_{i=1}^{m} \int_{L^{-1}(n_i)} \|x - n_i\|^2 \, d\mu.$$

Hence, we need to consider the pairs of different nuclei from N first. Let $n_i, n_j \in N$ such $n_i \neq n_j$ and denote $R_i = L^{-1}(n_i)$ and $R_j = L^{-1}(n_j)$ for simplicity. Since θ must be orthogonal to the line through n_i and n_j, it is defined as

$$\{x \in \mathbb{R}^d : \langle x, n_j - n_i \rangle = \beta\} \text{ for } \beta \in \mathbb{R}.$$

Let us consider $R_i \cup R_j$ and separate it using θ into $\mathcal{P}$ and $\mathcal{T}$. Since $\mu(R_j) = C_j$ and $\mu(R_i) = C_i$, we can find $\beta \in \mathbb{R}$ for which $\mu(\mathcal{P}) = C_i$ and $\mu(\mathcal{T}) = C_j$. Since $\mu(\mathcal{P}) = C_i$ and $\mu(R_i) = C_i$, we see that

$$\mu(\mathcal{P} \setminus R_j) = \mu(\mathcal{P}) - \mu(\mathcal{P} \cap R_j) = \mu(R_j) - \mu(\mathcal{P} \cap R_j) = \mu(R_j \setminus \mathcal{P}).$$

For $x \in R_j \setminus \mathcal{P}$ we have $\langle n_j - n_i, x \rangle \leq \beta$, and for $x \in \mathcal{P} \setminus R_j$ we have $\langle n_j - n_i, x \rangle \geq \beta$. Therefore,

$$\int_{R_j \setminus \mathcal{P}} \langle n_j - n_i, x \rangle \, d\mu \leq \int_{\mathcal{P} \setminus R_j} \langle n_j - n_i, x \rangle \, d\mu. \tag{1.5}$$

We also see that

$$R_j \cup R_i = \mathcal{P} \cup \mathcal{T} \Rightarrow R_j \cup R_i \setminus \mathcal{P} = \mathcal{T} \Rightarrow R_j \setminus \mathcal{P} = \mathcal{T} \setminus R_i. \tag{1.6}$$

Moreover, we have

$$R_j \setminus \mathcal{P} = R_j \setminus (R_j \cap \mathcal{P}) \text{ and } R_i \setminus \mathcal{T} = R_i \setminus (R_i \cap \mathcal{T}). \tag{1.7}$$

By combining (1.6) and (1.7), the inequality (1.5) becomes

$$\int_{R_j} \langle n_j, x \rangle \, d\mu + \int_{R_i} \langle n_i, x \rangle \, d\mu \leq \int_{\mathcal{P}} \langle n_j, x \rangle \, d\mu + \int_{\mathcal{T}} \langle n_i, x \rangle \, d\mu. \tag{1.8}$$

Since $\mu(R_i) = \mu(\mathcal{P}) = C_i$, $\mu(R_j) = \mu(\mathcal{T}) = C_j$ and $R_i \cup R_j = \mathcal{P} \cup \mathcal{T}$, (1.8) is equivalent to

$$\int_{\mathcal{P}} \|x - n_j\|^2 \, d\mu + \int_{\mathcal{T}} \|x - n_i\|^2 \, d\mu \leq \int_{R_j} \|x - n_j\|^2 \, d\mu + \int_{R_i} \|x - n_i\|^2 \, d\mu.$$

Therefore, using $\mathcal{P}$ and $\mathcal{T}$ we can reconstruct $R_j \cup R_i$. Furthermore, $\mathcal{P}$ and $\mathcal{T}$ fulfill the hyperplane condition and do not increase the value of (1.4). Since N is finite, we can reconstruct the assignment L fully, which yields the lemma.

□

With a less comprehensive proof, the last lemma is stated as Observation 1 in Aurenhammer et al. [1998], p. 65.

Remark. By Lemma 3, we see that if the least-square assignment subject to some capacity constraint exists, it is realized by a set of convex polyhedra $\{P_i\}_{i=1}^m$. Those polyhedra are defined in the following manner

$$P_j = \bigcap_{i=1, i\neq j}^{m} \theta_{ji}.$$

We see that each P_j is defined as a finite intersection of closed half-spaces in $\mathbb{R}^d$. Thus, P_j forms a convex polyhedron in $\mathbb{R}^d$.

Next, we show that the least-square assignment subject to capacity constraint C exists. We need to clarify some geometrical concepts and define a tiling in $\mathbb{R}^d$ first. The following two definitions come from Aurenhammer [1987], p. 49.

Definition 8. *Let us consider $j \in \mathbb{N}$ such that $0 \leq j \leq d$. A j-polyhedron is a convex subset of dimension j of $\mathbb{R}^d$ that can be expressed as the intersection of a finite number of closed half-spaces in $\mathbb{R}^d$. The boundary of a j-polyhedron P, denoted by ∂P, consists of finitely many i-polyhedra, called i-faces of P, for $i < j$.*

Definition 9. *A tiling T of a nonempty set $X \subseteq \mathbb{R}^d$ is a finite collection of j-polyhedra for which:*

i, the union of the j-polyhedra of T is equal to X,

ii, the relative interiors of the j-polyhedra of T pairwise do not intersect.

Remark. For our purposes, when dealing with capacity constraints on the unit cube, we are interested in d-polyhedra (cells) and $(d-1)$-polyhedra (cell faces). Such a tiling of $\mathbb{R}^d$ is a particular case of a tessellation.

Lemma 4. *Let us consider C from Definition 7, μ from Definition 5 and the class of assignments $\mathbb{R}^d \to N$ realized by the set of convex polyhedra $\{P_i\}_{i=1}^m$ with the following properties:*

i, $\{P_i \cap [0,1]^d\}_{i=1}^m$ defines a tiling of $[0,1]^d$,

ii, $\mu(P_i) = C_i,\ i = 1, \ldots, m$,

iii, each P_i has fewer than m k-faces,

where $k = d - 1$. Then this class of assignments contains a least-square assignment $L\colon \mathbb{R}^d \to N$ subject to C.

Proof. The proof of this lemma can be found in Aurenhammer et al. [1998], p. 66, as the proof of what the authors called Lemma 3.

□

1.2 Realizability

Lemma 4 shows that the least-square assignment L subject to capacity constraint C exists. We need to show that it can be realized as a Laguerre tessellation for some set of nuclei N and weights W. Therefore, we introduce a concept of an orthogonal dual of a tiling of $\mathbb{R}^d$, which helps us distinguish when a tiling of $\mathbb{R}^d$ can be realized as a Laguerre tessellation.

Definition 10. *Let T be a tiling of $\mathbb{R}^d$ and let $\mathcal{D}(T)$ be a finite set of points in $\mathbb{R}^d$. We call $\mathcal{D}(T)$ the orthogonal dual of T if it satisfies the following conditions:*

i, $\mathcal{D}(T)$ contains exactly one point $p_i \in \mathbb{R}^d$ for each member M_i of T such that distinct points correspond to distinct members,

ii, for distinct members M_i and M_j of T a line connecting the corresponding points p_i and p_j is orthogonal to $M_i \cap M_j$,

iii, any ray parallel to the line connecting p_i and p_j, directed from p_i to p_j, and intersecting both M_i and M_j, first meets M_i.

Having defined an orthogonal dual of a tiling of $\mathbb{R}^d$, we can determine whether the tiling is realized as a Laguerre tessellation.

Theorem 5. *A tiling T of $\mathbb{R}^d$ can be realized as a Laguerre tessellation for some set of nuclei N in $\mathbb{R}^d$ and weights W in $\mathbb{R}$ if and only if an orthogonal dual of T exists.*

Proof. The proof of this theorem can be found in Aurenhammer [1987], p. 52–54, as the proof of what the author called Lemma 4 (formulated in terms of power diagrams and generalized spheres).

□

Theorem 5 allows us to prove Claim 1 by combining the results from Aurenhammer et al. [1998], p. 67–68, and Aurenhammer [1987], p. 52.

Theorem 6. *Let us consider N, μ and C from Definition 7. Then there exists a set W of real numbers (weights) such that*

$$\mu(reg_W(n_i)) = C_i,\ i = 1, \ldots, m.$$

Proof. From Lemma 4, we know that there exists a least square assignment $L\colon \mathbb{R}^d \to N$ realized by a set of convex polyhedra $\{P_i\}_{i=1}^m$ such that $\{P_i \cap [0,1]^d\}_{i=1}^m$ defines a tiling of $[0,1]^d$ and $\mu(P_i) = C_i$, $i = 1, \ldots, m$.

It is enough to show that the convex tiling that defines the least-square assignment L subject to the capacity constraint C has an orthogonal dual. The proof of this part can be found in Aurenhammer et al. [1998], p. 67, as the proof of what the authors called Lemma 4.

□

Remark. By taking ρ to be the probability density function of the uniform distribution on $[0,1]^d$, μ becomes the Lebesgue measure on $[0,1]^d$. Hence, for $d = 3$, we can decompose the unit cube into convex polyhedra of prescribed volumes.

1.3 Weight Vector

In the following part, we prove that the assignment induced by the Laguerre tessellation of $\mathbb{R}^d$ with nuclei N and weights W gives rise to a concave function that admits minimizers. We require a few definitions for the simplicity of notation.

Definition 11. *Let us consider N and W from Definition 1 and μ from Definition 5. For an arbitrary Borel measurable assignment $A\colon [0,1]^d \to N$ we define a function $f_A\colon \mathbb{R}^m \to \mathbb{R}$ as*

$$f_A(W) = \int_{[0,1]^d} \rho(x)\ p_W(x, A(x))\ dx,\ W \in \mathbb{R}^m,$$

the vector of capacities from the assignment A as $B(A) = (\mu(A^{-1}(n_i)))_{i=1}^m$ and a function Q, called the value of A, as

$$Q(A) = \int_{[0,1]^d} \rho(x)\ \|x - A(x)\|^2\ dx.$$

All concepts from the last definition were introduced in Section 5 of Aurenhammer et al. [1998], p. 70–71. Next, we prove that f_A is linear in W.

Lemma 7. *Let f_A be the function from Definition 11. Then f_A is a linear function in W.*

Proof. Let $\mathbb{I}_X$ be the characteristic function of $X \subseteq \mathbb{R}^d$. Let us consider ω as defined in the proof of Lemma 2 and denote the elements of W by w_i. Then

$$f_A(W) = \int_{[0,1]^d} \rho(x)\ \|x - A(x)\|^2\ dx - \int_{[0,1]^d} \rho(x)\ \omega(A(x))\ dx,$$

which is equal to

$$Q(A) - \int_{[0,1]^d} \rho(x)\ \omega(A(x))\ dx.$$

Hence, it suffices to prove that

$$\int_{[0,1]^d} \rho(x)\ \omega(A(x))\ dx = \langle B(A), W\rangle.$$

By linearity of the Lebesgue integral, we see that

$$\int_{[0,1]^d} \rho(x)\ \omega(A(x))\ dx = \int_{[0,1]^d} \rho(x) \sum_{i=1}^m \mathbb{I}_{A^{-1}(n_i)}(x)\ \omega(n_i)\ dx,$$

which becomes

$$\sum_{i=1}^m \int_{A^{-1}(n_i)} \rho(x)\ w_i\ dx = \sum_{i=1}^m w_i\ \mu(A^{-1}(n_i)),$$

which is equal to $\langle W, B(A)\rangle$. Thus,

$$f_A(W) = Q(A) - \langle W, B(A)\rangle.$$

□

Remark. Without proof, Lemma 7 is stated in Aurenhammer et al. [1998], p. 71.

For each weight vector $W \in \mathbb{R}^m$ we find A_W and use it as a parameter for f_A. We prove that the resulting function has specific beneficial properties.

Theorem 8. *Let us consider f_A from Lemma 7. Let $f\colon \mathbb{R}^m \to \mathbb{R}$ be a function on the weight space defined as*

$$f(W) = f_{A_W}(W) = Q(A_W) - \langle B(A_W), W\rangle,\ W \in \mathbb{R}^m.$$

Then f is a concave and continuous function in W with gradient $-B(A_W)$ at W.

Proof. Throughout the proof, we work on a probability space (Ω, Σ, μ), where we put $\Omega = [0,1]^d$ and $\Sigma = \sigma(\Omega)$.

(i) Continuity

First, we prove that f is continuous on $\mathbb{R}^m$. Let us consider a sequence $\{W_k\}_{k=1}^{\infty}$ in $\mathbb{R}^m$ such that $W_k \to W,\ k \to \infty$. We aim to show that

$$f(W_k) \to f(W),\ k \to \infty. \tag{1.9}$$

From (1.9), it then follows that f is continuous at W. To prove (1.9) it suffices to show that

$$Q(A_{W_k}) \to Q(A_W),\ k \to \infty$$

and

$$B(A_{W_k}) \to B(A_W),\ k \to \infty.$$

Let us consider all points in $\mathbb{R}^d$ at the same power distance p_W from two different nuclei in N and denote it by E. We see that

$$E = \{x \in \mathbb{R}^d :\ \exists (n_i, n_j) \in N :\ n_i \neq n_j,\ p_W(x, n_i) = p_W(x, n_j)\},$$

or equivalently

$$E = \bigcup_{j \neq i} \{x \in \mathbb{R}^d :\ p_W(x, n_i) = p_W(x, n_j)\}.$$

For a fixed $j \neq i$ we consider

$$\{x \in \mathbb{R}^d :\ p_W(x, n_i) = p_W(x, n_j)\}$$

and we see that it is equivalent to

$$\{x \in \mathbb{R}^d :\ \|n_i\|^2 - \|n_j\|^2 + w_j - w_i = 2\langle x, n_i - n_j\rangle\}.$$

Since the set N and weights w_i, w_j are fixed and $n_i \neq n_j$, the last expression defines a hyperplane in $\mathbb{R}^d$. Hence, E is a finite union of hyperplanes in $\mathbb{R}^d$. We know that μ is absolutely continuous with respect to λ^d. Since λ^d-measure of a hyperplane in $\mathbb{R}^d$ is zero, we have $\mu(E) = 0$ from the subadditivity of measures.

Let us consider $E' = \Omega \cap E$ and $x \in \Omega \setminus E'$. Then there exists some $n_i \in N$ such that $A_W(x) = n_i$. Since $x \notin E$, we get

$$\forall j \neq i :\ \|x - n_i\|^2 - w_i < \|x - n_j\|^2 - w_j. \tag{1.10}$$

Let $j \in \{1, \ldots, m\}$ for which we have $j \neq i$. Then $\|x - n_i\|^2 - \|x - n_j\|^2$ is a constant $D_j \in \mathbb{R}$. We see that (1.10) becomes

$$\forall j \neq i : \ w_j < w_i - D_j.$$

Then there exists $\delta_j > 0$ such that for all $h \in (-\delta_j, \delta_j)$ we have

$$w_j + h < w_i - D_j.$$

Let us consider $\delta = \min_{j \neq i} \delta_j$. Then $\delta > 0$ and for all $j \neq i, \ h \in (-\delta, \delta)$ we have

$$\|x - n_i\|^2 - w_i < \|x - n_j\|^2 - (w_j + h).$$

Hence, there is a nonempty neighborhood of W in $\mathbb{R}^m$, on which $Z \to A_Z(x)$ is a constant function. Since $W_k \to W, \ k \to \infty$, there exits $k_0 \in \mathbb{N}$ such that for $k \geq k_0$, vectors W_k stay in the above-mentioned neighborhood, i.e.,

$$\forall k \geq k_0 : \ A_{W_k}(x) = n_i \Rightarrow A_{W_k}(x) \to A_W(x), \ k \to \infty.$$

We know that

$$Q(A_W) = \int_\Omega \|x - A_W(x)\|^2 \, d\mu(x).$$

Let us consider Q as a function of W for A_W. Then we have $Q \colon \mathbb{R}^m \to \mathbb{R}$ and

$$Q(W) = \int_\Omega \|x - A_W(x)\|^2 \, d\mu(x). \tag{1.11}$$

Since the integrand in (1.11) is bounded by one and $A_{W_k} \to A_W, \ k \to \infty$ μ-almost everywhere, we use the Lebesgue theorem to obtain

$$\lim_{k \to \infty} Q(W_k) = \int_\Omega \lim_{k \to \infty} \|x - A_{W_k}(x)\|^2 \, d\mu(x) = Q(W). \tag{1.12}$$

Furthermore, let us consider B as a vector function of W for A_W. Then we have $B \colon \mathbb{R}^m \to \mathbb{R}^m$ and

$$B(W)_j = \int_\Omega \mathbb{I}_{[A_W(x) = n_j]} \, d\mu(x), \ j = 1, \ldots, m. \tag{1.13}$$

We see that the integrand in (1.13) is bounded by one. Since $A_{W_k} \to A_W, \ k \to \infty$ μ-almost everywhere, we use the Lebesgue theorem to obtain

$$\lim_{k \to \infty} B(W_k)_j = \int_\Omega \lim_{k \to \infty} \mathbb{I}_{[A_{W_k}(x) = n_j]} \, d\mu(x) = B(A_W)_j, \ j = 1, \ldots, m. \tag{1.14}$$

Therefore, by combining (1.12) and (1.14), we get

$$\lim_{k \to \infty} f(W_k) = \lim_{k \to \infty} Q(W_k) - \langle B(W_k), W_k \rangle = Q(W) - \langle B(W), W \rangle.$$

Hence, f is continuous at W. Since W was arbitrary, f is continuous on $\mathbb{R}^m$.

In the following part, we adapt the proof of a similar statement, Theorem 1.1, in Kitagawa et al. [2019], p. 2613, to show the differentiability and concavity of f.

(ii) Concavity

We prove that the superdifferential of f at W contains $-B(W)$. Let us consider $W, V \in \mathbb{R}^m$. Then we have

$$f(V) + \langle -B(V), W - V \rangle = f(V) + \langle B(V), V \rangle - \langle B(V), W \rangle, \tag{1.15}$$

which is equal to

$$Q(V) - \langle B(V), W \rangle = f_{A_V}(W).$$

Since f minimizes f_A over all Borel measurable $A \colon \mathbb{R}^d \to N$ at W, we see that

$$f_{A_V}(W) = Q(V) - \langle B(V), W \rangle \geq Q(W) - \langle B(W), W \rangle = f(W). \tag{1.16}$$

By combining (1.15) and (1.16), we have

$$\forall W, V \in \mathbb{R}^m : \ f(V) + \langle -B(V), W - V \rangle \geq f(W).$$

Since f is continuous on $\mathbb{R}^m$ and $\partial^+(V) \neq \emptyset, \ V \in \mathbb{R}^m$, then f is concave on $\mathbb{R}^m$.

(iii) Gradient

Let us consider the set of all sequence $\{W_k\}_{k=1}^{\infty}$ in $\mathbb{R}^m$ converging to W such that f is differentiable at W_k and denote it by T. By Theorem 25.6 from Rockafellar [1970], we know that $\partial^+ f(W)$ is equal to

$$\mathrm{conv}\Big\{ \lim_{k \to \infty} \nabla f(W_k) : \{W_k\}_{k=1}^{\infty} \in T \Big\}. \tag{1.17}$$

Since B is continuous on $\mathbb{R}^m$, then (1.17) is identical with

$$\mathrm{conv}\Big\{ \lim_{k \to \infty} -B(W_k) : \{W_k\}_{k=1}^{\infty} \in T \Big\} = \{-B(W)\}.$$

Hence, f is differentiable on $\mathbb{R}^m$ and

$$\forall W \in \mathbb{R}^m : \ \nabla f(W) = -B(W).$$

□

Remark. Let us consider a function $h \colon \mathbb{R}^m \to \mathbb{R}$ on the weight space defined as

$$h(W) = -\langle C, W \rangle - f(W), \ W \in \mathbb{R}^m, \tag{1.18}$$

where $C \in \mathbb{R}^n$ is the given capacity constraint vector. By Theorem 8, we see that h is a continuous convex function on $\mathbb{R}^m$ with the gradient at W equal to

$$\nabla h(W) = B(A_W) - C.$$

If we satisfy the capacity constraint for some weight vector $W^* \in \mathbb{R}^m$, then

$$B(A_{W^*}) = C \Rightarrow \nabla h(W^*) = 0,$$

which means that any extremum of h on $\mathbb{R}^m$ corresponds to such W^*.

1.4 Centroidal Tessellations

In the following section, we work on $(\mathbb{R}^d, \mathcal{B}^d, \mu)$ for $\mu = \lambda^d$ restricted to $[0,1]^d$. Hence, the definition of the capacity of a cell in Laguerre tessellations coincides with the definition of a d-dimensional volume. First, we define the centroid of a subset of $\mathbb{R}^d$.

Definition 12. *Let $X \in \mathcal{B}^d$ such that $\mu(X) \neq 0$. Then we define the centroid of X as a vector $\boldsymbol{t} \in \mathbb{R}^d$ such that*

$$\boldsymbol{t} = \frac{1}{\mu(X)} \int_{\mathbb{R}^d} \boldsymbol{x}\, \mathbb{I}_X(\boldsymbol{x})\; d\mu(\boldsymbol{x}),$$

where $\mathbb{I}_X$ is the characteristic function of X.

Remark. Since we only consider Laguerre tessellations with positive capacities in our application, we can always compute the centroids of their cells.

Next, we define a particular case of a Laguerre tessellation, the centroidal Laguerre tessellation.

Definition 13. *Let us consider a Laguerre tessellation of $\mathbb{R}^d$ with nuclei N and weights W from Definition 4 such that its cells, denoted by $B_1, \ldots, B_m$, have nonzero capacities. We call this tessellation centroidal if each nucleus n_i is the centroid of B_i for $i = 1, \ldots, m$.*

Remark. In the proof of Theorem 8, we have seen that the set of all points at the same power distance from two different nuclei has μ-measure 0. Therefore,

$$\mu(A_W^{-1}(n_i)) = \mu(B_i),\ i = 1, \ldots, m.$$

Hence, it does not matter whether we base the definition of the centroidal Laguerre tessellation on Definition 3 or Definition 4.

Based on the theoretical results from the previous sections, we can find a set of weights W for a set of nuclei N in $\mathbb{R}^d$ such that the Laguerre tessellation of $\mathbb{R}^d$ with nuclei N and weights W realizes the prescribes capacity constraint C.

We want to find a centroidal Laguerre tessellation with the prescribed capacity constraint C. To find this tessellation, we use a simple iterative approach called the Lloyd-type centering from Kuhn et al. [2020], p. 118. The idea behind this method is to compute the Laguerre tessellation for a given set of nuclei and capacities and then use its cells' centroids as the nuclei in the next iteration.

2. Application

In the following chapter, we describe the algorithm for iterative computation of the weights for a finite set of nuclei N such that the resulting Laguerre tessellation has the prescribed capacities. Furthermore, we comment on the characteristics of the algorithm and its convergence. All figures used in this chapter were created using R software, see R Core Team [2021].

2.1 Algorithm

Let us define $C \in \mathbb{R}^m$ as the prescribed capacity vector for the set of m nuclei N in $\mathbb{R}^d$. Let us also denote by C_k the vector of capacities resulting from the assignment A_{W_k} for $W_k \in \mathbb{R}^m$ and $k \in \mathbb{N}_0$. We know that the function h, as defined in (1.18), on the weight space $\mathbb{R}^m$ is convex continuous and

$$\nabla h(W_k) = C_k - C,\ W_k \in \mathbb{R}^m,\ k \in \mathbb{N}_0.$$

We want to find a vector $W^* \in \mathbb{R}^m$ such that $\nabla h(W^*) = 0$. Since h is convex on its domain, we look for a global minimum of h on $\mathbb{R}^m$. We use the following gradient descent

$$W_{k+1} = W_k - \alpha_k \nabla h(W_k) = W_k - \alpha_k(C_k - C),\ k \in \mathbb{N}_0,$$

where we set $\alpha_0 = 0.1$ and W_0 as a zero vector in $\mathbb{R}^m$. We define the step size as

$$a_k = \frac{\langle W_k - W_{k-1}, W_k - W_{k-1}\rangle}{\langle C_k - C_{k-1}, W_k - W_{k-1}\rangle},\ k \in \mathbb{N},$$

which is called the Barzilai-Borwein method and is mentioned in Kuhn et al. [2020], p. 121. To compute the next iteration W_{k+1}, we require W_k, W_{k-1} and C_k, C_{k-1}. We see that

$$W_1 = W_0 - \alpha_0(C_0 - C) = \alpha_0(C - C_0),$$

where C_0 is the vector of capacities for W_0, i.e., for the Voronoi tessellation of $\mathbb{R}^d$ with nuclei N. We can compute the capacity vector C_1 using W_1. Hence, we are prepared to compute all subsequent iterations.

We have defined our iterative method, the step size choice, and the initial values. Next, we need to establish the formula for examining the accuracy of a solution. We use the same criterion as in Kuhn et al. [2020]. We say that the iterative method has reached prescribed accuracy at the iteration number k if

$$R_1(k) = \frac{\|C_k - C\|}{\min_{1\le i\le m} C_i} \le 0.01,\ k \in \mathbb{N}_0. \tag{2.1}$$

We see that we sum the differences between the capacities in the iteration number k and the prescribed capacities. Then we normalize it by the smallest prescribed capacity not to diminish the effect of the smaller cells.

We want to use the specialized library Voro++ to compute the vector of capacities in each iteration. However, the program operates with the so-called radii $r_i^2 = w_i,\ i = 1, \dots, m$ instead of the weights w_i. Let us define

$$\kappa = \min_{1 \le i \le m} w_i, \text{ and } r_i = \sqrt{w_i - \kappa},\ i = 1, \dots, m.$$

We see that for $x \in \mathbb{R}^m$ and $n_i, n_j \in N$ we have

$$\|x - n_i\|^2 - w_i \le \|x - n_j\|^2 - w_j \iff \|x - n_i\|^2 - r_i^2 \le \|x - n_j\|^2 - r_j^2.$$

Hence, the sets which define the cells of a Laguerre tessellation with weights w_i and the sets which define the cells of a Laguerre tessellation with radii r_i are equivalent. Therefore, we can use both weights w_i and radii r_i to generate precisely the same Laguerre tessellation with the same vector of capacities.

2.2 Convergence

In our application, we work on $(\mathbb{R}^3, \mathcal{B}^3, \mu)$ with $\mu = \lambda^3$ restricted to $[0,1]^3$. We generate the positions of the nuclei in $[0,1]^3$ from $\mathrm{U}(0,1)$, uniform distribution on $(0,1)$, for each coordinate. To generate the prescribed capacities we employ three different distributions. First, as in Kuhn et al. [2020], p. 124, we set

$$C_i = \frac{1}{m} \text{ for } i = 1, \dots, m, \tag{2.2}$$

where the capacities are homogeneously distributed. Next, we set

$$C_i = \frac{U_i}{\sum_{j=1}^m U_j} \text{ for } U_i \sim \mathrm{U}(0,1),\ i = 1, \dots, m. \tag{2.3}$$

We see that $\mathbb{E}C_i = 1/m$ in both cases; however, the second one is not deterministic. Hence, it should bring more irregularities into our samples. Finally, to see how the algorithm performs under significant variability of capacities, we use

$$C_i = \frac{E_i}{\sum_{j=1}^m E_j} \text{ for } E_i \sim \mathrm{Exp}(2),\ i = 1, \dots, m, \tag{2.4}$$

where $\mathrm{Exp}(2)$ denotes the exponential distribution with a mean value of $1/2$. We test our implementation by increasing the number of nuclei from 100 nuclei to 1000 nuclei with a step increase of 100. We then summarize the results in Table A.1.

In Table A.1, we see that the number of iterations generally increases with the number of nuclei, except for a few cases. We believe those irregularities are caused by the non-monotonic convergence of the algorithm, see Figure A.1. We also observe that the number of iterations for the most basic example (100 nuclei) increases from the first row to the third. We believe this follows from the fact that the algorithm needs more iterations to reach a more diverse sample of prescribed capacities.

Next, we examine one particular case and plot the residual (2.1) to see whether the algorithm approaches the solution monotonically. We generate a sample of 500 nuclei in $[0,1]^3$ with coordinates from $\mathrm{U}(0,1)$ and equal capacities. We increase the prescribed accuracy to 10^{-10} in (2.1). Then the algorithm finds a solution in 739 iterations with the accuracy of $9.02 \cdot 10^{-11}$.

In Figure A.1, we plot the number of iterations n against the common logarithm of residual value in each iteration $\log_{10} R_1(n)$ for the first 739 iterations. We see that at first (up to $n = 100$), the algorithm approaches the solution monotonically. However, after iteration 100, the convergence becomes wildly different while following the downward trajectory.

Remark. We want to comment that, generally, the convergence of the Barzalia-Borwein gradient descent method is not guaranteed by any theoretical results. In each case, we assume that it converges, as the authors did in Kuhn et al. [2020], p. 121.

2.3 Effect of Variance

In the previous part, we explored the convergence behavior of our implementation of the Barzilai-Borwein gradient descent. Next, we examine the algorithm's behavior while gradually varying the underlying variance of the prescribed capacity sample.

As in the previous part, the coordinates of nuclei in $[0,1]^3$ come from $\mathrm{U}(0,1)$. To explore the variance, we generate the capacities from a normalized Gamma distribution. Let us consider $X_i \sim \Gamma(\tau, \eta)$ for $\tau, \eta > 0$, where $\Gamma(\tau, \eta)$ denotes the Gamma distribution with parameters τ, η. We know that

$$\mathbb{E}X_i = \tau\eta \text{ and } \mathrm{var}X_i = \tau\eta^2.$$

We set the mean value to unity, thus $\eta = \tau^{-1}$, because we are interested only in the variance. Then we generate random samples with 100, 200, 300, and 400 nuclei and capacities from

$$C_i = \frac{X_i}{\sum_{j=1}^{m} X_j}, \ i = 1, \ldots, m, \ X_i \sim \Gamma(\tau, 1/\tau) \tag{2.5}$$

for $\tau \in \{4,\ 2,\ 4/3,\ 1,\ 4/5,\ 2/3,\ 1/2\}$. Then the variance of X_i is equal to 0.25, 0.50, 0.75, 1.00, 1.25, 1.50, 2.00, i.e., it gradually increases.

We then observe the number of iterations the algorithm needed to reach prescribed accuracy (2.1) and present them according to the number of nuclei and the variance of the underlying distribution of capacities in Table A.2.

In Table A.2, we see that the number of interactions needed to reach prescribed accuracy generally increases with the number of nuclei. However, there are a few cases where the number decreases. We believe the non-monotonic convergence causes this, see Figure A.1. We also see that as the variance of the underlying distribution of capacities increases, the number of iterations also increases. There also are a few cases that do not fit the general trend. The results indicate that the convergence, as measured by the number of iterations, appears to depend strongly on the underlying variance of the capacity sample.

2.4 Lloyd-Type Centering

We approach a centroidal Laguerre tessellation in the following section using the Lloyd-type centering algorithm. The concept of centroidal Laguerre tessellations is presented in Definition 13, and the convergence of the Lloyd-type centering algorithm is reported by Bourne and Roper [2015], p. 2550. The Voro++ library carries out the computation of the centroids in a Laguerre tessellation.

Let us consider $\mu = \lambda^d$ restricted to $[0,1]^d$, a set of m nuclei N in $[0,1]^d$ and a prescribed capacity vector $C \in \mathbb{R}^m$. The solution of our method is the set of nuclei with the associated set of weights that realize a centroidal Laguerre tessellation subject to C.

We compute the Laguerre tessellation of $\mathbb{R}^d$ with nuclei N and constraint C using the algorithm from the previous sections. Then we compute the centroids of its cells and denote them by $\{t_1, \ldots, t_m\}$. We use those centroids as the nuclei for the next iteration.

In the iteration number k, for $k \in \mathbb{N}$, we compute the centroids of the cells of a newly computed Laguerre tessellation subject to the same capacity constraint C and denote them $\{t_1^k, \ldots, t_m^k\}$. We use the following residual criterion for examining the accuracy of a solution

$$R_2(k) = \sqrt{\sum_{i=1}^{m} C_i \|n_i - t_i^k\|^2} \leq 0.001, \ k \in \mathbb{N}. \tag{2.6}$$

We compute the squared Euclidean distance of the nuclei in the iteration number k and the centroids of a newly calculated Laguerre tessellation. Then we weight them by the prescribed capacity fractions C_i. Hence, we give preference to bigger cells. A similar approach is used in Kuhn et al. [2020], p. 124.

As in the previous section, we work with nuclei in $[0,1]^3$ whose coordinates come from $\mathrm{U}(0,1)$. However, in the case of a centroidal Laguerre tessellation, the nuclei of our solution will generally differ from the starting nuclei because the algorithm changes them in each iteration. First, we generate the prescribed capacities from the identical three distributions as in Section 2.2 and present the results in Table A.3.

In Table A.3, we see that the number of iterations generally decreases with the number of nuclei, except for a few cases. We think that this trend is caused by the fact that we increase the number of uniformly distributed nuclei in a finite unit cube and that centroidal Laguerre tessellations are quite regular. Hence, the algorithm needs fewer iterations to reach the solution. We believe that the non-monotonic convergence causes the irregularities, see Figure A.2.

We also observe that the number of iterations for the most simple case (100 nuclei) differs only slightly across three different underlying distributions. Thus, the number of iterations needed to reach prescribed accuracy for the Lloyd-type centering algorithm does not appear to depend on the variance of the underlying distribution of capacities as much as the Barzilai-Borwein gradient descent does.

Remark. Since we need to apply the Barzilai-Borwein gradient descent in each iteration of the Lloyd-type centering algorithm, the execution time is generally longer for the second algorithm.

Next, we explore a specific sample and plot the residual (2.6) to see whether the algorithm approaches the solution monotonically. We use the same example as in Section 2.2, i.e., a sample of 500 nuclei in $[0,1]^3$ with coordinates from $\mathrm{U}(0,1)$ and homogeneous capacities. We increase the accuracy to 10^{-6} in (2.6). Then the algorithm finds a solution in 1523 iterations with the precision of $9.98 \cdot 10^{-7}$.

In Figure A.2, we plot the number of iterations n against the common logarithm of residual value in each iteration $\log_{10} R_2(n)$ for the first 1523 iterations. At first, the algorithm approaches the solution monotonically. However, around the iteration number 100, the residual value varies wildly while still following the downward trend.

Finally, we examine the effect of the underlying variance of the capacity sample on the number of iterations as in Section 2.3. We work with the normalized Gamma distribution and generate the samples with the increasing underlying variance. We test the Lloyd type centering implementation for different values of τ and different number of nuclei as in Section 2.3. We then present the results in Table A.4.

In Table A.4, we see that the number of iterations decreases with the increasing number of nuclei. We also observe that the number of iterations does not appear to increase with the rising underlying variance of the capacity sample. Hence, the results suggest that the Lloyd-type centering might not be as dependent on the underlying variance of the capacity sample as the Barzilai-Borwein gradient descent.

Conclusion

This thesis aimed to study the concept of Laguerre tessellations and develop an algorithm for generating Laguerre tessellations with prescribed cell volumes. The problem of Laguerre tessellations has been studied for at least two centuries, and in the thesis, we followed the theoretical findings of Aurenhammer et al. [1998] and Kuhn et al. [2020].

In the introduction, we described two approaches to Laguerre tessellations and commented on their similarities and differences. Then we presented the main result of the thesis.

The first chapter explores the existence of Laguerre tessellations with prescribed volumes and demonstrates that those can always be realized. Then it describes the iterative method for numerically approaching Laguerre tessellations. In addition, we introduced the concept of a centroidal Laguerre tessellation and the algorithm for generating centroidal Laguerre tessellations with prescribed cell volumes.

The second chapter describes the application of the algorithms as mentioned earlier. Then it explores the convergence using the number of iterations needed to reach prescribed accuracy as the main characteristic. Furthermore, we explored the relationship among the number of iterations, the number of nuclei, and the variance of the underlying distribution of the prescribed cell volume sample. Moreover, we discussed the Lloyd-type centering algorithm for computing centroidal Laguerre tessellations with prescribed cell volumes.

We want to highlight our direct contributions to distinguish between the theory in the literature and our work. We proved Lemma 2, expanded the proof of Lemma 3, and proved Lemma 7 and Theorem 8. Moreover, we implemented the Barzilai-Borwein gradient descent algorithm and the Lloyd-type centering algorithm in C++.

We believe that the main contribution of the thesis is the systematic study of Laguerre tessellations from the definition to their numerical generation. There are two crucial observations arising from our application. First, the Barzilai-Borwein gradient descent converged in all examples, as in Kuhn et al. [2020]. Since there is no theoretical guarantee for convergence, this is surprising. Second, increasing the number of nuclei or the variance of the underlying distribution of the prescribed cell volume sample raises the number of iterations for the Barzilai-Borwein gradient descent. However, increasing the number of nuclei does not seem to increase the number of iterations for the Lloyd-type centering.

Bibliography

F. Aurenhammer. A criterion for the affine equivalence of cell complexes in $\mathbb{R}^d$ and convex polyhedra in $\mathbb{R}^{d+1}$. *Discrete & Computational Geometry*, 2:49–64, 1987.

F. Aurenhammer, F. Hoffmann, and B. Aronov. Minkowski-Type Theorems and Least-Squares Clustering. *Algorithmica*, 20:61–76, 1998.

D. P. Bourne and S. M. Roper. Centroidal Power Diagrams, Lloyd's Algorithm, and Applications to Optimal Location Problems. *SIAM Journal on Numerical Analysis*, 53:2545–2569, 2015.

J. Kitagawa, Q. Mérigot, and B. Thibert. Convergence of a Newton algorithm for semi-discrete optimal transport. *Journal of the European Mathematical Society*, 21:2603–2651, 2019.

J. Kuhn, M. Schneider, P. Sonnweber-Ribic, and T. Böhlke. Fast methods for computing centroidal Laguerre tessellations for prescribed volume fractions with applications to microstructure generation of polycrystalline materials. *Computer Methods in Applied Mechanics and Engineering*, 369:113–175, 2020.

C. Lautensack and S. Zuyev. Random Laguerre Tessellations. *Advances in Applied Probability*, 40:630–650, 2008.

R Core Team. *R: A Language and Environment for Statistical Computing*. R Foundation for Statistical Computing, Vienna, Austria, 2021.

R. T. Rockafellar. *Convex Analysis*, volume 28 of *Princeton Mathematical Series*. Princeton University Press, Princeton, NJ, 1970.

C. H. Rycroft. VORO++: A three-dimensional Voronoi cell library in C++. *Chaos: An Interdisciplinary Journal of Nonlinear Science*, 19:041111, 2009.

A. Attachments

A.1 Figures

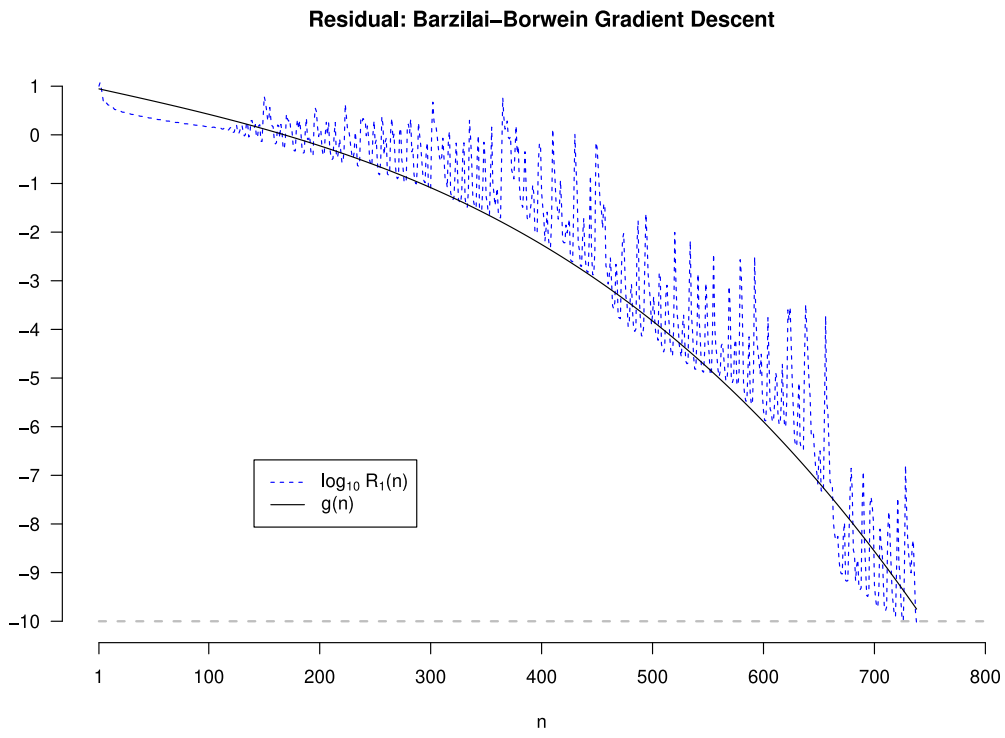

Figure A.1: Convergence behaviour of the Barzilai-Borwein gradient descent for $m = 500$ and homogeneous prescribed capacities, R_1 in (2.1). For illustration $g(n) = an^3 + bn^2 + cn + d$, where $a = -1.58 \cdot 10^{-8}$, $b = -1.21 \cdot 10^{-6}$, $-5 \cdot 10^{-3}$ and $d = 0.95$.

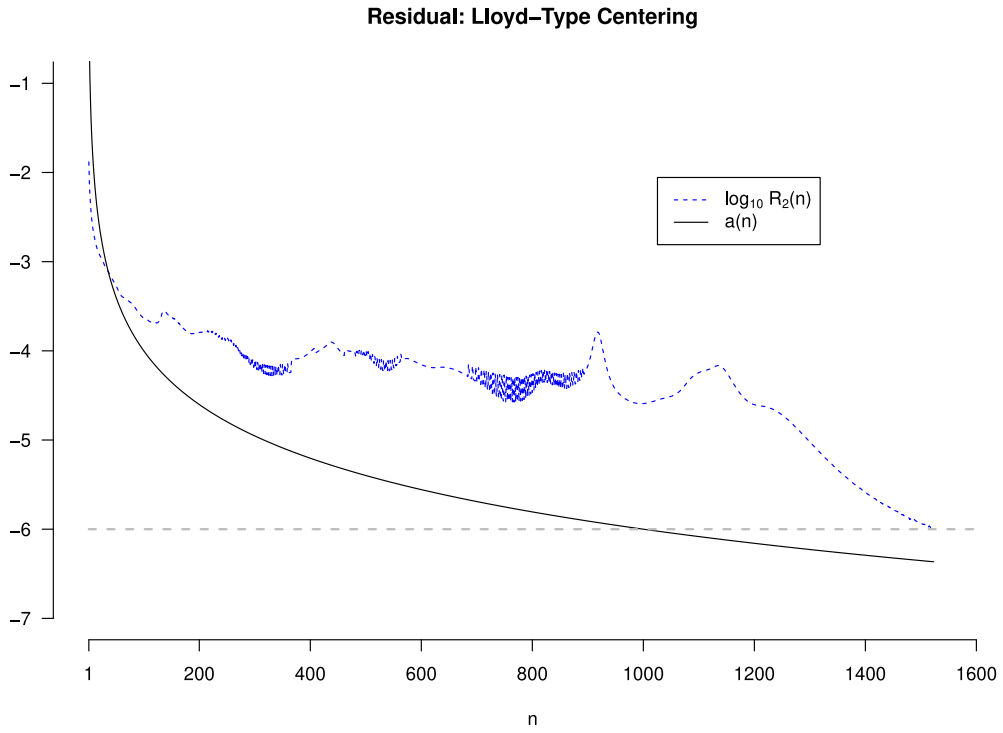

Figure A.2: Convergence behaviour of the Lloyd-type centering algorithm for $m = 500$ and homogeneous prescribed capacities, R_2 in (2.6). For illustration $a(n) = -2\log_{10}(n)$.

A.2 Tables

	m	100	200	300	400	500	600	700	800	900	1000
H		54	134	174	339	395	349	387	445	424	436
U		91	153	205	250	301	307	330	629	594	1491
E		309	271	1495	1485	1208	1227	2880	5027	3441	4698

Table A.1: Barzilai-Borwein gradient descent. The iteration counts for different numbers of nuclei from 100 to 1000 and different underlying distributions of capacities: H for homogeneous, U for U$(0, 1)$, and E for Exp(2), see (2.2)–(2.4).

τ^{-1}	**m**	100	200	300	400
0.25		84	119	208	205
0.50		106	126	217	242
0.75		68	136	234	305
1.00		282	235	268	365
1.25		272	817	1411	818
1.50		436	1125	1457	1287
2.00		962	2157	3229	2329

Table A.2: Barzilai-Borwein gradient descent. The iteration counts for different numbers of nuclei from 100 to 400 and distinct values of variance τ^{-1}, see (2.5).

	m	100	200	300	400	500	600	700	800	900	1000
H		45	36	30	27	28	24	22	21	20	20
U		60	49	33	27	32	27	26	22	22	20
E		43	46	43	32	28	27	25	24	25	22

Table A.3: Lloyd-type centering. The iteration counts for different numbers of nuclei from 100 to 1000 and different underlying distributions of capacities: H for homogeneous, U for U$(0, 1)$, and E for Exp(2), see (2.2)–(2.4).

τ^{-1}	**m**	100	200	300	400
0.25		43	37	35	27
0.50		35	35	36	26
0.75		43	33	33	27
1.00		48	46	30	30
1.25		54	35	35	31
1.50		62	43	42	32
2.00		43	40	36	34

Table A.4: Lloyd-type centering. The iteration counts for different numbers of nuclei from 100 to 400 and distinct values of variance τ^{-1}, see (2.5).

A.3 Electronic Attachment

We provide the data sets and the algorithms used in the application in the electronic attachment to the thesis. All implementations are written in C++ and use the specialized C++ library Voro++.

All data sets are stored in `PTS` directory. The implementations of the algorithms discussed in the thesis are stored in `PRG` directory. We implemented the Barzilai-Borwein gradient descent algorithm for Laguerre tessellations in $[0,1]^3$, stored in `BB.txt`. We also implemented the Lloyd-type centering algorithm for Laguerre tessellations in $[0,1]^3$, stored in `LC.txt`. Additionally, we provide a piece of software for generating data sets compatible with both implementations, stored in `RSG.txt`.